

9C.3 ASSESSING THE IMPACT OF TOTAL PRECIPITABLE WATER AND LIGHTNING ON SHIPS FORECASTS

John Knaff* and Mark DeMaria

NOAA/NESDIS Regional and Mesoscale Meteorology Branch, Fort Collins, Colorado

John Kaplan

NOAA/AOML Hurricane Research Division, Miami, Florida

Jason Dunion

CIMAS, University of Miami – NOAA/AOML/HRD, Miami, Florida

Robert DeMaria

CIRA, Colorado State University, Fort Collins, Colorado

1. INTRODUCTION

This study is motivated by the potential of two rather unique datasets, namely measures of lightning activity and Total Precipitable Water (TPW), and their potential for improving tropical cyclone intensity forecasts.

The plethora of microwave imagers in low earth orbit the last 15 years has made possible the regular monitoring of water vapor and clouds over the earth's oceanic areas. One product that has much utility for short-term weather forecasting is the routine monitoring of total column water vapor or TPW.

In past studies lower environmental moisture has been shown to inhibit tropical cyclone development and intensification (Dunion and Velden 2004; DeMaria et al 2005, Knaff et al 2005). The delay or lack of intensification of TC surrounded by dry environments is often accompanied by moderate vertical wind shears. In the Atlantic the TPW has been used to examine the modification of the mean tropical sounding associated with the Saharan air layer and mid-latitude dry air intrusions (Dunion and Marron 2008; Dunion 2010). TPW has also been shown to be well related to the underlying sea surface temperature on relatively long time scales, as

would be anticipated from the Clausius-Clapeyron relationships (Stephens 1990).

The TPW is typically estimated by its relationship with certain passive microwave channels ranging from 19 to 37 GHz (Kidder and Jones 2007). These same channels, particularly 19GHz in the inner core region, have been related to tropical cyclone intensity change (Jones et al 2006). TPW fields also offer an excellent opportunity to monitor real-time near core atmospheric moisture, which like rainfall (i.e. 19GHz) is related to intensity changes as modeling studies of genesis/formation suggest that saturation of the atmospheric column is coincident or precede rapid intensification (Nolan 2007).

In addition to the availability of real-time TPW data, long-range lightning detection networks now offer the addition of continuous cloud to ground lightning detection in the remote oceanic regions. There is also increased interest in lightning relationships as the next generation geostationary satellite system starting with GOES-R will include a geostationary lightning mapper (GLM). The GLM will provide nearly continuous times and locations of total lightning with an accuracy of about 10 km over most of the field of view of GOES-east and – west. This coverage will include nearly all of the regions where tropical cyclones occur in the Atlantic and north Eastern Pacific. This lightning data will provide new and unique information that is related to the deep convective structures, including those of tropical cyclones, and the current long-range lightning detection networks

*Corresponding author address: John Knaff, NOAA NESDIS, RAMMB, CIRA, Colorado State University, Campus Delivery 1375, Fort Collins, 80523-1375, USA; e-mail: John.Knaff@NOAA.gov

offer an opportunity to better understand how lightning activity is related tropical cyclone intensification well before GOES-R is launched.

Previous studies that made use ground-based lightning networks have revealed a number of interesting relationships between storm structure and the lightning distribution. Using data from the National Lightning Detection Network (NLDN) Molinari et al. (1999) have shown that the lightning density (strikes per unit area and time) tends to have a bi-modal structure as a function of radius from the storm center, with maxima near the eyewall region and in the rainband region (150-300 km radius) and a minimum in between. Their study and more recent analysis with the Long-range Lightning Detection Network (LLDN) (Squires and Businger 2008) indicate that the lightning near the storm center tends to be much more transient than that in the rainband region. Squires and Businger (2008) also indicated that there was a long lived peak lighting density in the core associated with peak intensity of both Rita and Katrina in 2005. Corbosiero and Molinari (2002) showed a strong relationship between the environmental shear and the azimuthal distribution of lightning, with a maximum in strikes on the down shear side of the storm.

Using the very simple argument that lightning is favored when the cloud updrafts are stronger (e.g., Black and Hallet 1999) it might be expected that increased lightning activity near the storm center would be correlated with short-term intensification. However, previous studies with the NLDN and LLDN data have shown that this relationship is not straightforward, with peaks in lightning density occurring during the intensification, steady state and weakening stages of tropical cyclones. Black and Hallet (1999) showed that the vertical electric fields in tropical cyclones are much weaker than those in continental convection suggesting that lightning outbreaks in the tropical cyclone inner core might be somewhat rare – this result was confirmed by Cecil and Zipser (1999).

More recently, DeMaria and DeMaria (2009) calibrated World Wide Lightning Location Network data (Rodger et al 2006) and used it along with several years of tropical cyclone environmental data in the Atlantic to show that 1) the effect of

vertical wind shear complicates the relationship between lightning density and tropical cyclone intensity changes, 2) in a large sample, the lightning density minimum between inner core and rainband regions is averaged out, 3) inner core lightning density was only weakly related to intensity change while lightning density in the rainband regions was positively and significantly correlated to future intensity changes, and 4) that if vertical shear is accounted for there was a potential to improve statistical intensity forecasts using real-time lightning data such as will be provided by GLM.

In this study we will examine the statistical relationships between tropical cyclone intensity change and the location, variability and distribution of lightning and TPW. To do this we will make used the developmental databases and statistical model formulation of the Statistical Hurricane Intensity Prediction Scheme (DeMaria et al. 2005). Previous studies offer guidance as to where these new data may be most useful and where interdependencies with the environmental factor should also be accounted for. The following section will discuss datasets, methods, results, conclusions and future plans.

2. DATASETS

Six hourly TPW data comes from two sources. For the period 1995 – 2008, the TPW product was developed by Remote Sensing Systems (RSS) and uses a unified, physically based algorithm to estimate atmospheric water vapor from highly calibrated microwave radiometers. The water vapor values from SSM/I (DMSP constellation), TMI (TRMM) and AMSR-E (Aqua) instruments are combined to create composite maps four times per day and are derived using the following microwave channels: 19/22/37 GHz (SSM/I), 19/24/37 GHz (AMSR-E), 19/21/37 GHz (TMI). The description of the algorithms used can be found in Alishouse et al. (1990), Wentz (1997) and Wentz and Meissner (2000). To produce a more complete composite map in the earlier years, the maps consist of 12-hour averages in 1995, while in later years, a 6-hour average is produced (1996 to 2008). A time-weighted average of the satellite water vapor retrievals falling within a given 0.25

degree cell is produced. Empty cells are spatially filled using a 9x9 moving window and remaining holes are filled using satellite data from the map before or after (this essentially makes the map a +/- 9 hour data set though one can access the +/- 3 hour data). Any remaining small holes are again spatially filled using a 9x9 window. Information on filling process is retained. The resulting maps are over 99.8% complete for years after 2002.

A second TPW dataset, one produced in real time at NESDIS, which blends/overlays SSMI-based and AMSU-based TPW over the oceans with GPS-based TPW over the CONUS was used to extend the TPW dataset through 2009. The use of this product will also enable future real-time/operational products. This 12-hourly blending method is described in Kidder and Jones (2007). The algorithms for both the SSMI and AMSU are different than those used by the NRL TPW dataset. The SSMI data first utilizes the Alishouse et al. (1990) algorithm but then applies a correction described in Ferraro et al. (1996). The algorithm for the AMSU-based TPW is described in Ferraro and Co-authors (2005). Using the overlapping 2008 datasets a correction to the NESDIS TPW (i.e. so it has similar properties) was developed by binning NESDIS TPW with respect to the NRL TPW into 1 mm bins. The correction (1) makes use of the binned data through 52 mm (because NRL TPW seems to saturate at values close to 60 mm and limits the utility of the fit at the high end). Figure 1 shows the results of applying (1) to the data.

$$(1) \quad TPW_{corrected} = 1.165TPW_{NESDIS} - \left[\frac{TPW_{NESDIS}}{17.381} \right]^2$$

Lightning location and timing, mostly of Cloud-to-Ground (CG) lightning, is provided by the World Wide Lightning Location Network (WWLLN). The method uses VLF (3–30 kHz) radiation from a lightning stroke. The stable propagation and low attenuation of VLF waves in the earth–ionosphere waveguide allows a wide spacing of receiver sites of several thousand kilometers. Global lightning is located by using the time of group arrival. The dispersed waveform of the lightning impulse is processed at each receiving site. There are

currently 40 receiving station that provided global monitoring of CG lightning (see Dowden et al 2002 and Rodger et al. 2004).

The WWLLN data does not however detect all lightning and the data must be calibrated for use in our study. This calibration of the lightning density to climatology was described in DeMaria and DeMaria (2009) and has been updated through the 2009 season. The detection percentage for 2008 and 2009 in the Atlantic and (East Pacific) were found to be 6.0% (6.6%) and 14.7% (20.0%), respectively.

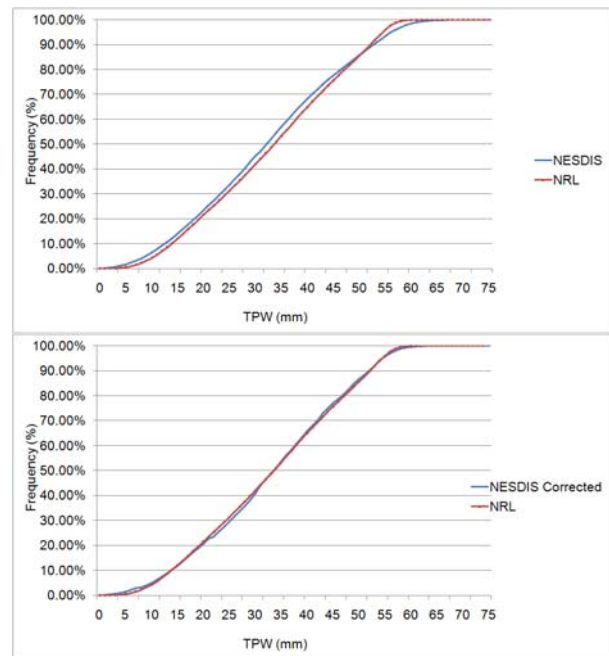


Figure 1. Cumulative probability distribution of the NESDIS TPW (blue) and the NRL TPW (red) before correction (top) and after the correction (1) is applied (bottom).

3. METHODOLOGY

A utilitarian approach is used in this study. The SHIPS statistical-dynamical model (DeMaria et al 2005) has shown intensity forecast skill by currently using 22 predictors to make forecasts of tropical cyclone intensity change. The predictors used are based on a 1982-2008 dataset that includes climatological/storm specific and dynamical predictors. This forms the basis for potential improvements offered in this study where

we seek to improve the current operational capabilities by the addition of information (i.e., predictors) related to variation of TPW and of lightning activity. Previous studies will also be used to guide our examination of these two datasets.

Case studies and observational evidence for the influence of vertical wind shear on tropical cyclone structure/intensity change suggests that TPW variations, particularly dry anomalies near the TC center can disrupt eyewall convection of mature tropical cyclones and inhibit convection in developing TCs (Dunion and Velden 2004). Furthermore, there is observational evidence that the influences of low TPW anomalies can be enhanced or modulated when combined with vertical wind shear. Most recently, modeling studies have shown that environmental moisture variability is related to TC size variations (Hill and Lackmann 2009) and those are likely related to other structural changes including intensity (Xu and Wang 2010). Stephens (1990) showed that as would be expected due to Clausius – Clapeyron relationships that TPW is well related to SST above 15°C, we will make use of this relationship as TCs move over a variety of different SST conditions.

For the purposes of this study, annuli and circular area averages and standard deviations at 200 km increments from the TC center will be examined for their utility of improving intensity forecasts. These quantities will also be modified by SSTs and vertical wind shear predictors to elicit the most robust predictive information.

Previous studies of lightning have show that lightning primarily occurs in two regions of the TC, namely in association with the eyewall and with the rainbands (Molinari et al 1999, DeMaria and DeMaria 2009). Furthermore, it appears that rainband lightning is related to intensity change in a positive manner and that eyewall lightning is more transient, but is related to short periods of rapid intensification and longer periods near peak intensity (Squires and Businger 2008). Lightning activity has also been shown to be nonlinearly related to variations of vertical wind shear (DeMaria and DeMaria 2009). Using these past findings we will examine lightning density (i.e., strikes per km² per year) and standard deviations

of lightning density in annuli and circular regions around the TC in 100 km increments; concentrating on those regions where lightning activity is known to occur. Again, there is an attempt to account for the affects of vertical wind shear and of current intensity in our statistical treatment of the data.

4. RESULTS

4.1 Atlantic TPW

As is the case for each potential predictor test a baseline forecast that includes all the times that TPW predictors were available is first produced using the standard 22 predictors of the SHIPS model. Using this “control” measure the dependent impact of each predictor combination can be tested.

Initial single predictor testing suggested that in two regions, 0 to 200 km and 200 to 600 km of the storm TPW may provide a predictive signal. As may have been anticipated greater and less variable (i.e. lower standard deviations) amounts of TPW favored intensification. Example of the TPW data centered on Hurricane Fred (2009) is shown in Fig. 2.

Attempts to include vertical wind shear information proved less successful than using TPW data alone. However accounting for SST variations did prove successful. To account for SST variation the equations developed in Stephens (1990) are exploited, where

$$(2) TPW_{SST} = 24.0e^{[0.064(SST-15)]}$$

provides an estimate of TPW [mm] based on the SST in degrees Celsius². A predictor then is created by subtracting TPW_{SST} , calculated by using the SST estimated at the TC center, from the observed value of TPW within 200km of the TC center. The greater the value of this predictor the greater the TPW value is relative to the local SST. The value of this predictor is +3.14 mm (SST=27.6C and TPW of 56.9) for Hurricane Fred

² Here a (r/1+γ) is assumed to be 0.22.

for the time shown in Fig 2. Fred continued to intensify for another 18 hours in an increasingly sheared environment.

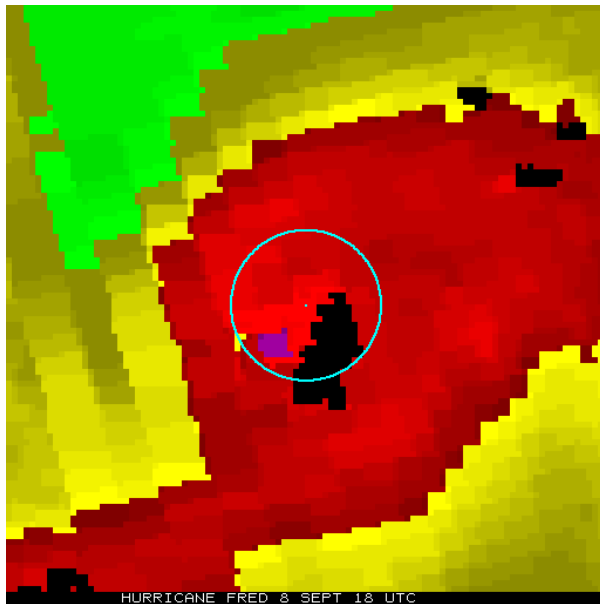


Figure 2. Corrected NESDIS TPW of Hurricane Fred 8 Sept 2009 at 18 UTC, (12N, 29.3W) is shown. The image is centered on the storm center and a 200km circle, centered on the storm, is provided for scale. The yellow to red interface and red to magenta interfaces represent 50 and 62.5 mm, respectively. Missing data (i.e., black) appears near the center, indicating rain contamination.

In addition to this 0-200km TPW-based predictor, the variability of the TPW over a larger circular area 0 to 600 km, measured as the area averaged standard deviation, was also found to be statistically significant. The value for our Fig. 2 example is 6.5 mm, indicating a likelihood of weakening. This treatment of the TPW data is similar to how infrared imagery – based predictors are also formulated.

To summarize the TPW findings in the Atlantic, the area averaged TPW from 0 to 200 km is a positive and statistically significant predictor for future hurricane intensity. This predictor can be improved slightly by parameterizing it as a TPW anomaly with respect to an expected climatological value given the local SST (DTPW).

The standard deviation of TPW 0 to 600km was also found to be a negative predictor (SD-TPW). Table 1 provides some relevant dependent statistics, which reveal that about an additional 0.3 to 0.7 % of the variance can be explained, but those improvements extend through 120h. It is also worth noting that while many attempts were made to combine vertical wind shear with measures of TPW, none resulted in improving the predictive capability over the predictors discussed above.

Table 1. Dependent statistics associated with the addition of TPW information to the Atlantic SHIPS model. Shown are the forecast hour, number of cases, variance explained from the control, variance explained with the addition of TPW predictors, and the p-values associated with those predictors.

Hour	Num	R ² Control	R ² TPW	P DTPW	P SD-TPW
6	5008	27.6	27.9	0.00	0.42
12	4708	35.1	35.6	0.00	0.02
24	4124	47.3	47.9	0.00	0.00
36	3618	55.1	55.6	0.00	0.00
48	317	60.6	61.2	0.00	0.00
72	2458	67.1	67.7	0.00	0.00
96	1917	69.6	70.3	0.00	0.00
120	1520	71.9	72.6	0.00	0.00

4.2 East Pacific TPW

Similar results with respect to TPW were found in the East Pacific basin. Dependent results show that the same predictors developed in the Atlantic work well in this basin. Very slight improvements in the percent variance explained can be obtained by using larger and/or smaller radii for the calculation of the SD-TPW predictor. In fact, a SD-TPW predictor calculated over an 800 km circle provided the best overall results. However since the improvements were rather small, the same predictors used in the Atlantic are used here. Table 2 shows the dependent statistics. Improvements in this basin are comparable with those found in the Atlantic.

Table 2. *Dependent statistics associated with the addition of TPW information to the East Pacific SHIPS model. Shown are the forecast hour, number of cases, variance explained from the control, variance explained with the addition of TPW predictors, and the p-values associated with those predictors.*

Hour	Num	R ² Control	R ² TPW	P DTPW	P SD-TPW
6	4903	45.9	46.1	0.00	0.04
12	4641	51.2	51.6	0.00	0.00
24	4225	56.9	57.5	0.00	0.00
36	3625	61.6	62.1	0.00	0.00
48	3164	65.8	66.5	0.00	0.00
72	2359	72.3	73.1	0.01	0.00
96	1711	76.4	77.0	0.03	0.00
120	1195	78.1	78.8	0.00	0.00

4.3 Atlantic Lightning

From the discussion of previous research above we anticipated that lightning density (strikes per km per year) would be potentially important near the eyewall and in the rainbands. Lightning densities and standard deviations of lightning density were again calculated in circular areas and annuli centered on the storm center, but with radial increments of 100km. A six hour window is used to collect lightning information.

Upon examining these potential predictors from the relatively large database, the rainband eyewall differences are smoothed out and as was found in DeMaria and DeMaria (2009). As a result most of the lightning predictive signal is associated with the inner region of the storm. Our findings suggest that the lightning density (LD) within circular areas within 100 and with 200km of the storm were most related to intensity changes. Both had inverse relationships with future intensification.

The scatter plots associated with LD vs. intensity change (not shown) suggested that the square root of LD had a more linear relationship with intensity change. Using this simple transformation the predictive utility of the LD was improved.

From previous studies the lightning density has also been shown to be a non-linear function of vertical wind shear. Multiplying our predictors, the square root of LD 0 to 100 km and 0 to 200 km, by the time averaged vertical wind shear between 850 and 200 hPa, also resulted in greater dependent variance being explained.

Finally, other authors have shown that lightning is a function of intensity. Namely that lightning density increase at or near peak intensity. To account for this affect the predictors were then multiplied by the current intensity. This resulted in a dramatic improvement in dependent variance explained.

Because the use of larger regions is felt to be more stable for these potentially operational results, we choose the larger area measure of lightning density to calculate potential improvements. Thus the final and only lightning related predictor is the square root of the 0 to 200 km LD times the current intensity times the time dependent vertical wind shear between 850 and 200 hPa. It is interesting to note that the resulting statistics suggest that inner region lightning is generally a negative factor when predicting intensity change, but if the vertical wind shear is relatively low (i.e., less than ~ (10) 15 kt) and the initial intensity is less than ~ (90) 60 kt, some limited lightning activity can occur without negative implications to the further intensification. Table 3 provides some relevant dependent statistics, which reveal that about an additional 3% of the variance for the 12h forecast can be explained with most improvements extend through 48h.

Table 3. *Dependent statistics associated with the addition of lightning information to the Atlantic SHIPS model. Shown are the forecast hour, number of cases, variance explained from the control, variance explained with the addition of lightning predictor (i.e., the LD 0 to 200 km times the current intensity times the time-dependent vertical wind shear 850 to 200 hPa), and the p-values associated with that predictor.*

Hour	Num	R ² Control	R ² LD- term	P LD- term
6	1471	26.7	29.5	0.00
12	1363	33.9	37.4	0.00
24	1155	47.0	49.9	0.00
36	984	54.4	57.4	0.00
48	840	59.6	61.7	0.00
72	629	70.2	71.2	0.00
96	470	76.6	76.7	0.32
120	352	84.6	84.6	0.73

4.4 East Pacific Lightning

Similar results with respect to lightning were found in the East Pacific basin. Dependent results indicate that the same predictors developed in the Atlantic work well in this basin, however the improvements in the SHIPS model were more modest and again mostly occurring for the 6-48h forecasts. This ~ 1% improvement vs. 3% in the Atlantic is likely due to much fewer storms beginning the extra-tropical transition and the fact that the SHIPS model already explains a greater amount of variance in this basin. Table 4 shows the dependent statistics.

Table 4. Dependent statistics associated with the addition of lightning information to the East Pacific SHIPS model. Shown are the forecast hour, number of cases, variance explained from the control, variance explained with the addition of lightning predictor (i.e., the LD 0 to 200 km times the current intensity times the time-dependent vertical wind shear 850 to 200 hPa), and the p-values associated with that predictor.

Hour	Num	R ² Control	R ² LD- term	P LD- term
6	1679	44.6	45.6	0.00
12	1579	49.5	50.6	0.00
24	1381	54.5	55.7	0.00
36	1194	59.4	60.7	0.00
48	1031	64.3	65.1	0.00
72	749	72.6	72.6	0.19
96	544	78.8	78.8	0.70
120	319	84.0	84.0	0.94

4.5 Combining TPW and Lightning

In previous sections we have presented the utility of using TPW and lightning information in the SHIPS modeling framework. In this section we briefly present dependent improvements that could be expected if both datasets were used in combination. Figure 2 shows the percent variance improvement that TPW and lightning data produces in both the Atlantic and East Pacific Basins based on our dependent dataset. The results suggest that an additional 4.1% (1.4%) of the variance could be explained by the 12 hour SHIPS forecasts in the Atlantic and (East Pacific) with similar improvements through 48 hours.

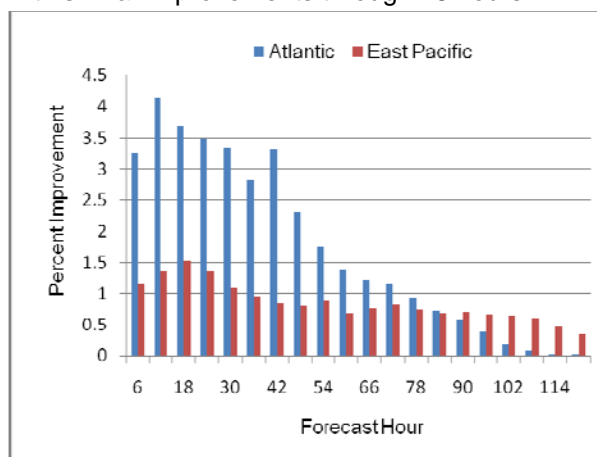


Figure 2. The combined percent variance improvement found by adding TPW and lightning based predictors described in the text to the SHIPS model (circa 2009).

5. CONCLUSIONS & FUTURE WORK

The conclusions of our present study are encouraging suggesting that there is potential utility of real-time TPW and lightning information for improving the existing SHIPS model forecasts. Results suggest that in the Atlantic the combination of such information could possibly improve forecasts significantly; explaining an additional three percent of the variance (or reduce the RMS errors 0.5 - 0.4 knots) in the 36 – 48 h forecast times. Most of the large improvements were the result of lightning information that improves the short term (0 to 48 h) forecasts the most. Findings show that the most important TPW information comes from the anomaly of near core

TPW vs. what the TPW likely should be given local SST and from the standard deviation TPW within 600km of the TC center. The lightning information is found to be most useful within 200km of the TC center. The general relationship is negative and can be improved by using information about the current intensity and the time-weighted vertical wind shear.

These relationships held up in the East Pacific, however the amount of additional variance explained was much less in that basin. This may be due to the rare occurrence of extra-tropical transition in this basin, which is often accompanied by electrification and strong vertical wind shear, but this is speculation. Figure 2 shows the anticipated improvements that are possible in the two basins.

With the results showing that both TPW and Lightning information help in the statistical forecasting of TC intensity change, future work will concentrate on statistical correction models that make use of these information. Those corrections would eventually be available to operations at NHC/CPHC. Previous studies concerning improvements to the Rapid Intensification Index (RII: Kaplan et al. 2010) – also discussed at this conference, have also shown the utility of TPW information to improve the discrimination of rapidly intensifying TC. The next logical task is to examine the utility of lightning information in the same capacity. We hope to have an experimental version of the RII that makes use of lightning information available by 1 August 2010 to be distributed during the GOES Proving Ground activities at NHC.

Acknowledgements: The authors wish to thank the World Wide Lightning Location Network (<http://wwlln.net>), a collaboration among over 40 universities and institutions, for providing the lightning location data used in this paper. Partial support for this study was provided by NOAA grant NA17RJ1228. The views, opinions, and findings contained in this report are those of the authors and should not be construed as an official National Oceanic and Atmospheric Administration or U.S. Government position, policy, or decision.

REFERECNCES

- Alishouse, J., S. Snyder, J. Vongsathorn, and R. Ferraro, 1990: Determination of oceanic total precipitable water from the SSM/I, *IEEE Trans. Geosci. Remote Sens.*, **28**, 811-816.
- Black., R.A., and J. Hallet, 1999: Electrification in hurricanes. *J. Atmos. Sci.*, **56**, 2004-2028.
- Cecil, D. J., and E. J. Zipser, 1999: Relationships between tropical cyclone intensity and satellite based indicators of inner core convection: 85-Ghz ice-scattering and lightning. *Mon. Wea. Rev.*, **127**, 103-123.
- Corbosiero, K.L., and J. Molinari, 2002: The effects of vertical wind shear on the distribution of convection in tropical cyclones. *Mon. Wea. Rev.*, **130**, 2110-2123.
- DeMaria, M. , R. DeMaria, 2009: Applications of lightning observations to tropical cyclone intensity forecasting. [16th Conference on Satellite Meteorology and Oceanography](#), Jan. 12-15, 2009, Phoenix, AZ 6pp.
- _____, M. Mainelli, L.K. Shay, J.A. Knaff, and J. Kaplan, 2005: Further Improvements in the Statistical Hurricane Intensity Prediction Scheme (SHIPS). *Wea. Forecasting*, **20**, 531-543.
- Dowden, R.L., Brundell, J.B.; Rodger, C.J. Source, 2002: VLF lightning location by time of group arrival (TOGA) at multiple sites, *Journal of Atmospheric and Solar-Terrestrial Physics*, **64**, 817-30
- Dunion, J.P., 2010: Re-Writing the Climatology of the Tropical North Atlantic and Caribbean Sea Atmosphere. *J. Climate*. (Accepted).
- _____, J. P. and C. S. Marron: 2008: A Reexamination of the Jordan Mean Tropical Sounding Based on Awareness of the Saharan Air Layer: Results from 2002. *J. Climate*, **21**: 5242-5253.
- _____, and C. S. Velden, 2004: The impact of the Saharan Air Layer on Atlantic tropical cyclone activity. *Bull. Amer. Meteor. Soc.* **90**, 353-365.
- Ferraro, R. R., F. Weng, N. C. Grody, and A. Basist, 1996: An eight year (1987-94) climatology of rainfall, clouds, water vapor, snowcover, and sea-ice derived from SSM/I measurements. *Bull. Amer. Meteor. Soc.*, **77**, 894-905.

- , and Coauthors, 2005: NOAA operational hydrological products derived from the Advanced Microwave Sounding Unit. *IEEE Trans. Geosci. Remote Sens.*, **43**, 1036–1049.
- Hill, K. A., and G. M. Lackmann, 2009: Influence of environmental humidity on tropical cyclone size. *Mon. Wea. Rev.*, **137**, 3294–3315.
- Jones, T. A., D. J. Cecil, and M. DeMaria, 2006: Passive Microwave-Enhanced Statistical Hurricane Intensity Prediction Scheme. *Wea. and Forecasting*, **21**, 613–635.
- Kaplan, J., M. DeMaria, and J.A. Knaff, 2010: A revised tropical cyclone rapid intensification index for the Atlantic and east Pacific basins. *Wea. Forecasting*, **25**, 220–241.
- Kidder, S.Q. and A.S. Jones, 2007: A blended satellite Total Precipitable Water product for operational forecasting. *Journal of Atmospheric and Oceanic Tech.* **24**, 74–81.
- Knaff, J.A., C.R. Sampson, M. DeMaria, 2005: An operational statistical typhoon intensity prediction scheme for the Western North Pacific. *Weather and Forecasting*, **20**: 4, 688–699.
- Molinari, J., P. Moore, and V. Idone, 1999: Convective structure of hurricanes revealed by lightning locations. *Mon. Wea. Rev.*, **127**, 520–534.
- Nolan, David S., 2007: What is the trigger for tropical cyclogenesis? *Aust. Meteorol. Mag.* , **56** , 241–266.
- Rodger, C.J., S. Werner, J.B. Brundell, E.H. Lay, N.R. Thompson, R.H. Holzworth, and R.L. Dowden, 2006: Detection efficiency of the VLF World-Wide Lightning Location Network (WWLLN): initial case study. *Ann. Geophys.*, **24**, 3197–3214.
- Squires, K., and S. Businger, 2008: The morphology of eyewall lightning outbreaks in two category 5 hurricanes. *Mon. Wea. Rev.* **136**, 1706–1726.
- Stephens, G. L., 1990: On the relationship between water vapor over the oceans and sea surface temperature. *J. Climate*, **3**:634–645.
- Wentz, F.J., 1997: A well-calibrated ocean algorithm for SSM/I. *J. Geophys. Res.*, **102**, 8703–8718.
- , and T. Meissner, 2000: AMSR Ocean Algorithm Theoretical Basis Document, Version 2. Remote Sensing Systems, Santa Rosa, CA.
- Xu, J., and Y. Wang: Sensitivity of tropical cyclone inner-core size and intensity to the radial distribution of surface entropy flux. *J. Atmos. Sci.*, in press.